Proceeding of the IEEE
International Conference on Robotics and Biomimetics
Dali, China, December 2019

Design and Kinematics of Cable-Driven Soft Module Coupled with Spring*

Jihong Yan, Peipei Shi, Zhidong Xu, Jie Zhao, *Member, IEEE*

***Abstract*—Soft robot has become a hot point because it has excellent adaptability and safety with environment. However, poor motion accuracy and low stiffness have limit its applications. This paper proposes a cable-driven soft module coupled with spring. It has compact structure, large range of motion, standard plug-and-connect connector, and can be easily assembled into a soft manipulator or a gripper. The kinematics of the module and modular manipulator are established based on the piece-wise constant curvature (PCC) method. The nonlinear friction of cables and the gravity of the modules have been analyzed to obtain an accurate model. Experiments on modules and manipulators with different sizes and stiffness have demonstrated its accuracy. The modules can reach a maximum bending angle of 180 °, and the error is within 2.5 °. The manipulators can reach a total bending angle more than 270 °, and the error does not exceed 5 °. Finally a gripper equipped with three modules is developed. It can grasp objects with different shapes, fragility and weights range from 1g to 0.43kg. It also demonstrates the good flexibility and load capacity of the module.**

I. Introduction

Soft materials have brought the benefits of complex environmental adaptability and interactive security to the soft robot. But poor accuracy and low stiffness have limited the applications of soft robots. Integrating rigid materials and flexible mechanisms is a most common method, such as the particle jamming, phase change materials, origami, kirigami structures and so on [1-3]. The spring, which is a common typical flexible mechanism, can also be used to improve the mechanical properties of soft robots. Furthermore, it has the same form of motion as soft module, stretching, shortening, bending and even rotating. Therefore, adding spring mechanism to the soft module can not only maintain the motion mode and highly freedom of the module, but also enhance its stiffness and load capacity. In addition to the structure design, the driving method is another important factor affecting its performance. The cable-driven method performs good in response speed, output torque and motion accurace. During 2012-2018, the BioRobotics Institute of Scuola Superiore Sant'Anna has developed a series of tendon-driven or hybrid pneumatic and tendon-driven soft manipulators [4-6]. Among them the 12-cable-driven soft bionic octopus manipulator can achieve section control. Modular design is also a good solution in practical applications. The modular design method is adopted by the manipulators developed by STIFF-FLOP project[7-8] and the V-SPA module[9]. The advantage is that different combinations can achieve different tasks in various situations.

Kinematic modeling is one of the key problem in the cable-driven soft manipulator. At present, most models are based on the PCC (Piece-wise Constant Curvature) assumption and the Cosserat theory. Federico et al. establish the kinematics and statics model based on the Cosserat theory and Euler-Bernoulli beam theory[5]. Then a PCS (Piece-wise Constant Strain) model is proposed to establish the kinematics and dynamics of the cable-driven manipulator[10]. Wang et al. establish the model based on the Cosserat theory and the Kelvin theory[11]. Most of the current modeling methods ignore the friction of the cable or the gravity. For more accurate modeling and control, the effect of friction and gravity should be introduced in the kinematics model.

This paper introduces a soft cable-driven module embedded with a flexible spring inside. The design and fabrication method are introduced in section II. In section III, an improved PCC method with considering the nonlinear friction and gravity is proposed for establishing a more accurate kinematics. In section IV, experiments on modules and manipulators are carried out to verify the accuracy of the kinematics model. Then a gripper equipped with 3 modules is developed to demonstrate the application of the module. The conclusion is in Section V.

II. Design and Fabrication

A. Module design

The module design is shown in fig.1. It consists of one cylindrical spring, two rigid connectors, silicon tubes, winding fibers and the silicone body. A central channel is designed to install stiffening mechanism or pass through electric wires of the equipped end effectors.

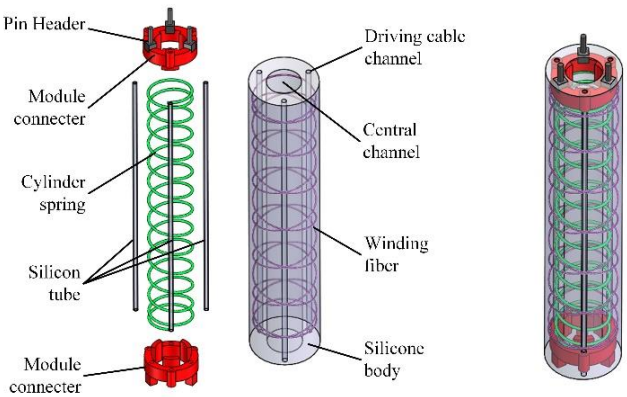

Fig. 1.The module design.

*Resrach supported by Self-Planned Task (SKLRS201804C) of State Key Laboratory of Robotics and System.

Jihong Yan is with State Key laboratory of Robotics and Systems, Harbin Institute of Technology, Harbin 150001, P. R. China (corresponding author to provide phone: 86-451-86413392; fax: 86-451-86413392; e-mail: jhyan@hit.edu.cn).

Peipei Shi, Zhidong Xu and Jie Zhao are with State Key laboratory of Robotics and Systems, Harbin Institute of Technology, Harbin 150001, P. R. China

978-1-7281-6321-5/19//$31.00 ©2019 IEEE

(a) Extension design of connectors

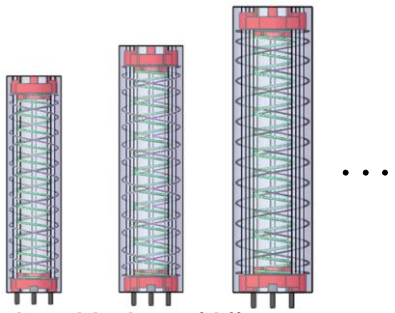

(b) Modules design of different sizes

Fig. 2 Modules design of different sizes.

The module has a soft outside but harder inside by adding a spring mechanism in the center of the silicone part. And modules can be easily assembled trough plug-and-connect method.Modules of different sizes are designed by extending the connectors, which is shown in Fig. 2. This design method makes it easy to be connected and extended.

B. *Fabrication*

As shown in fig.3, the fabrication processes can be divided into several steps: (1) cover the copper rods with silicone tubes; (2) assemble the rigid parts; (3) pour the elastomer silicone into the mold; (4) wind fiber on the silicone cylinder; (5) form a thin layer outside the module.

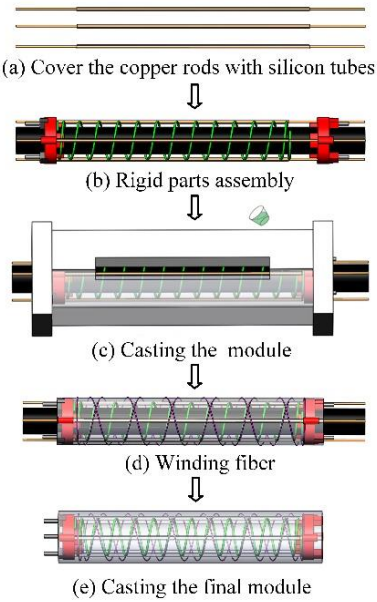

Fig. 3 The fabrication processes of the module.

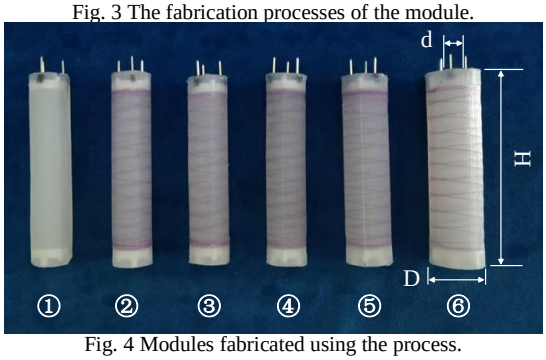

Fig. 4 Modules fabricated using the process.

According to the fabrication processes, a series of modules are fabricated into different specifications. The modules are shown in fig.4. And the main parameters are listed in table I.

TABLE I. THE PARAMETERS OF DIFFERENT MODULES

	Different parameters of the series modules		
Module number	**Module size** ***(D ×d ×H, mm³)***	**Spring size** ***(L ×Ds ×ds ×n, mm³)***	**Weight** ***(g)***
①	14×7×60	No spring	9.0
②	14×7×60	50×10×0.4×14	9.2
③	14×7×60	50×10×0.5×14	9.4
④	14×7×60	50×10×0.6×14	9.9
⑤	16×7×60	50×10×0.5×14	12.0
⑥	18×7×60	50×10×0.5×14	15.7
⑦	14×7×85	70×10×0.5×14	12.1

In table I, ***D*** is the diameter of the module, ***d*** is the diameter of the central channel of the module, ***H*** is the height of the module, ***L*** is the height of the spring, ***Ds*** is the diameter of the spring, ***ds*** is the wire diameter of the spring, ***n*** is the number of the spring coil. In addition, some parameters are measured. The friction coefficient between the cables and the silicone tubes is 0.3. The elastic modulus of the silicone is 0.11Mpa. The maximum bending angle is 180 °.

C. *Soft manipulator reconfiguration*

The modules can be assembled into series manipulator, which is shown in fig.5. In theory, modules can be connected infinitely. Different modules can be assembled into different manipulators, which is shown in the Fig.6. The cables pass through the near-end module to the remote module. One cable can control the bending of all modules, but there is coupling motion between modules. Modules of different sizes can also be connected. *N* modules can be connected in sequence by the diameter. The manipulator is controlled by 3n cables. Because of the coupling motion between modules, the complexity of its modeling and control will increase exponentially.

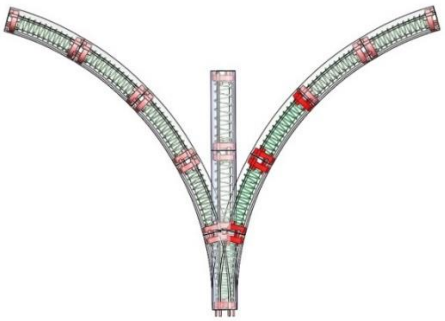

Fig. 5. Bending motion of the manipulator

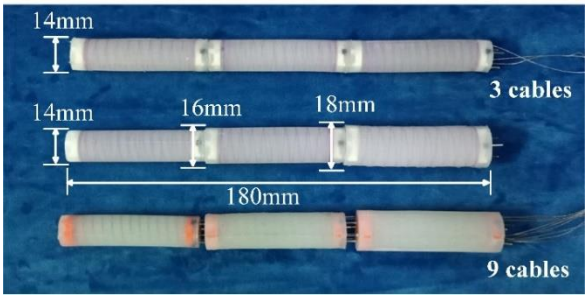

Fig. 6. Manipulators with different connection strategies

III. KINEMATICS

The PCC (piecewise constant curvature) model is used in the kinematics modeling of modules and manipulators proposed in this paper. Some non-negligible force including gravity and friction, are considered into the kinematics. The relationship between external force and deformation is established by the deformation energy and the Castigliano theorem.

A. Force analysis of the module

The module is subjected to external force including driving force of the cable, friction between cables and silicone tubes, and gravity. These forces work together to cause the module's bending motion, which is shown in fig.7(a) and fig.7(b). And the force analysis is shown in fig.7(c). The module is assumed as an arc.

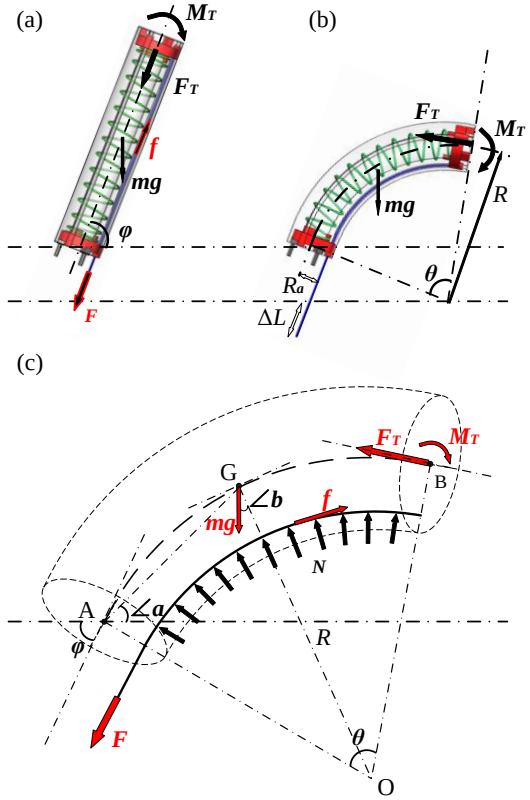

Fig. 7. Force analysis of a single module

During the modeling of the module, F is the driving force of the cable, f is the friction between the cable and silicon tube, μ is the friction coefficient, F_T is the actual driving force, M_T is the bending moment generated by the cable, φ is the initial attitude angle, θ is the bending angle, R is the arc radius of the bending module, R_a is the distance between the cable and the central axis of the module, m is the module's weight, ΔH is the compression of the module alone the central axis.

The cable is also bending to an arc. To analysis the friction, first divided the arc into n parts with equal length. Then set the tension on both sides of the i-th part to be F_i and F_{i+1}. f_i is the friction of the i-th part. k_i is the normal pressure density between the i-th cable and the silicone.

$$F_{i+1} = F_i + f_i = F_i + \frac{l}{n}\mu k_i = F_i - \frac{l}{n}\mu\frac{F_i}{R} \tag{1}$$

Then tension of each part of cable is proportional to series.

$$F_T = \lim_{n\to\infty} F\left(1-\frac{l\mu}{nR}\right)^n = Fe^{-\mu\theta} \tag{2}$$

From the Equation (2), it can be inferred that f is a nonlinear force. And the friction has a great influence on the module's driving force, especially when the bending angle θ is large. Because when the bending angle becomes larger, the positive pressure between the cable and the module also becomes larger.

The gravity will produce a bending moment, which can be written as Equation (3).

$$M_G = 2mgR\sin\frac{\theta}{4}\cos\left(\varphi-\frac{\theta}{4}\right) \tag{3}$$

B. Modeling of the spring

The spring compresses and bends following the module. First assume that the spring is subjected to a force F_a, and a bending moment M_a. The relationship between the bending angle and moment can be obtained by the Equation (5) [12]. The relationship of compression and pressure follows Hooke's law.

$$F_a = K\cdot\Delta H \tag{4}$$

$$\theta = n\pi M_a R_s\left(\frac{1}{E_a I_a}+\frac{1}{GI_P}\right) \tag{5}$$

In the equation, K is the spring constant; n is the number of the spring coil; R_s is the diameter of the spring; I_a is the area moment of inertia; I_p is the torsional moment of inertia; E_a is elastic modulus of the spring; G is shear module of the spring.

C. Modeling of the soft part

The deformation energy of the silicone body can be divided into two parts, the compression potential energy U_p and the bending potential energy U_b.

$$\begin{cases} U_p = \frac{1}{2}(\frac{\Delta H}{H})^2 EA \\ U_b = \frac{1}{2}(\frac{\theta}{H-\Delta H})^2 EI \end{cases} \tag{6}$$

According to the Castigliano theorem, the force F_b and the bending moment M_b can be obtained.

$$\begin{cases} F_b = \frac{\Delta H}{H}EA \\ M_b = \frac{\theta}{H-\Delta H}EI \end{cases} \tag{7}$$

D. Kinematics of the module

The module's deformation is generated by the combination of cable's driving force, module's gravity and friction. The effect of gravity on module's compression is negligible. Then the Equation (8) can be obtained.

$$\begin{cases} F_T = F_a + F_b \\ F_T R_a + M_G = M_a + M_b \end{cases} \tag{8}$$

By combining the Equation (2~8), the compression and bending angle of the module can be solved.

$$\begin{cases} \theta = \dfrac{R_a e^{-\mu\theta} F + M_G}{\dfrac{1}{n\pi R_s[\dfrac{1}{E_a I_a} + \dfrac{1}{GI_P}]} + \dfrac{EI}{H - \Delta H}} \\ \Delta H = \dfrac{e^{-\mu\theta} F}{K + \dfrac{EA}{H}} \end{cases} \tag{9}$$

E. Kinematics of the manipulator

The force analysis of the series manipulator is shown in fig.8. Compared to the force analysis of a single module, the ***i-th*** module ($1 \leq i$) has additional force from the following modules. The influence of the following module's gravity can be divided into a force $\boldsymbol{F_{Zi}}$ and a moment $\boldsymbol{M_{Zi}}$.

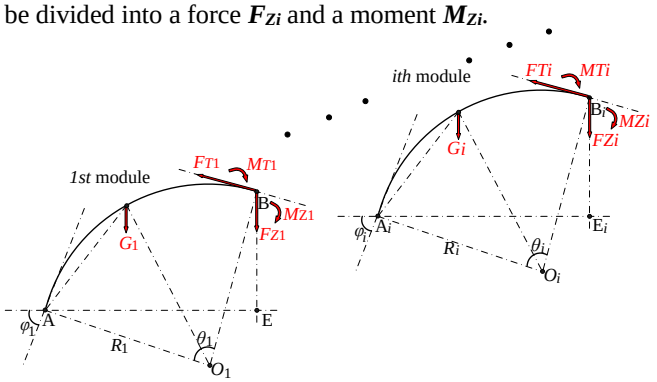

Fig. 8. Force analysis of the series manipulator

In fig.8, $\boldsymbol{F_{Ti}}$ is the driving force from cables; $\boldsymbol{M_{Zi}}$ is the moment generated by cables; $\boldsymbol{G_i}$ is the gravity of the ***i-th*** module; $\boldsymbol{\theta_i}$ is the bending angle of the ***i-th*** module; $\boldsymbol{\varphi_i}$ is the initial attitude angle of the ***i-th*** module.

$$\begin{cases} M_{Zi-1} - M_{Zi} = F_{Zi} R_i \sin(\dfrac{\theta_i}{2}) \cos(\varphi_i - \dfrac{\theta_i}{2}) + M_{Gi} \\ F_{Zi} = \sum_{k=i+1}^{n} [m_k g] \\ M_{Gi} = m_i g \left[(R_i - r_i) \sin(\varphi_i - \dfrac{\theta_i}{2}) + \dfrac{R_i \theta_i}{2} \cos(\varphi_i - \dfrac{\theta_i}{2}) \right] \\ \varphi_{i+1} = \varphi_1 - \sum_{k=1}^{i} \theta_k \end{cases} \tag{10}$$

The total bending moment of the module is set to be $\boldsymbol{M_i}$.

$$\begin{cases} M_i = M_{Zi-1} + M_{Ti} \\ M_{Zi-1} = \sum_{k=i}^{n} \left[F_{Zk} R_k \sin(\dfrac{\theta_k}{2}) \cos(\varphi_k - \dfrac{\theta_k}{2}) + M_{Gk} \right] \\ M_{Ti} = \sum_{k=i}^{n} [F_k e^{-\mu(\theta_1 + \ldots + \theta_k)} r_k] \end{cases} \tag{11}$$

The kinematics of the ***i-th*** module can be obtained by the Equation (12).

$$\begin{cases} \theta_i = \dfrac{M_i}{\dfrac{1}{n\pi R_{ki}[\dfrac{1}{E_1 I_1} + \dfrac{1}{G_1 I_P}]} + \dfrac{EI}{H_i - \Delta H_i}} \\ \Delta H_i = \dfrac{\sum_{k=i}^{n} [F_k e^{\mu(\theta_1 + \ldots + \theta_k)}]}{K_i + \dfrac{EA_i}{H_i}} \end{cases} \tag{12}$$

The final bending angle θ of the manipulator can be expressed as the Equation (13).

$$\theta = \sum_{1}^{n} \theta_i \tag{13}$$

IV. Experiment and Discussion

The experiments are divided into two parts, which are respectively deployed around the modules and the series manipulators.

A. Experiment on modules

The experimental platform is shown in fig. 9. The module is fixed on the 3D printing base. The driven cable is connected to a dynamometer. The dynamometer is attached to a ball screw. Rotating the handle can drive the dynamometer and the cable for linear motion. At the same time the module will perform bending motion.

The module ① and ② are used to test on the difference before and after adding a spring in the module. A plate is used to fix them. And the same force is applied to both the modules. The experiment result is shown in fig. 10. A partial collapse occurs in the bending motion of the module ①. This leads to the instability of its motion and the difficulty to achieve motion control. But after adding a spring into the module, the module ② can bend into a normal continuous arc. The spring acts to limit the radial deformation of the module. It is speculated that the spring disperses the local stress concentration of the silicon body.

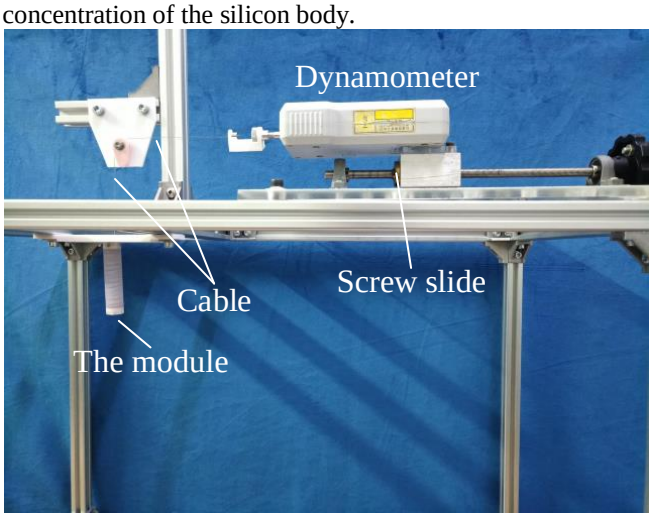

Fig. 9 The experiment setup

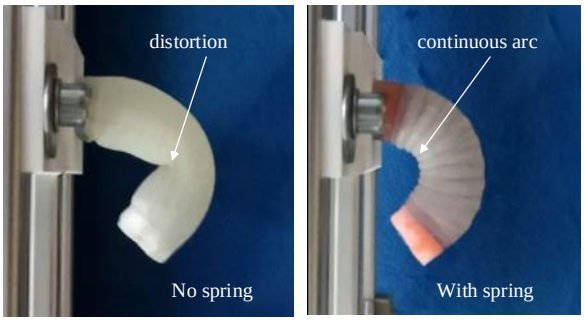

(a) bending of the module ① (b) bending of the module ②

Fig. 10. Difference of bending motion by adding a spring mechanism.

The spring in the cable driven soft modules is similar to the effect of fibers on pneumatic modules. Its function is to limit the radial deformation of the module and improve module rigidity. Adding a spring into the module can not only enhance stiffness, but also increase the stability of module's motion.

The module ②, ③,④ are used to test the kinematics proposed in section Ⅲ. The bending process of the module is shown in fig.11. And the experiment result is shown in fig.12. The experiment results is very close to the theoretical value. Within the range from 0 to 180 °, the maximum error of modules ②, ③, ④ are 2.41 °, 2.35 °, 2.46 °, respectively. The error does not exceed 2.5 °. The effectiveness of the module kinematics can be demonstrated by the results.

Fig. 11 Bending motion of the module (0 to 180 °).

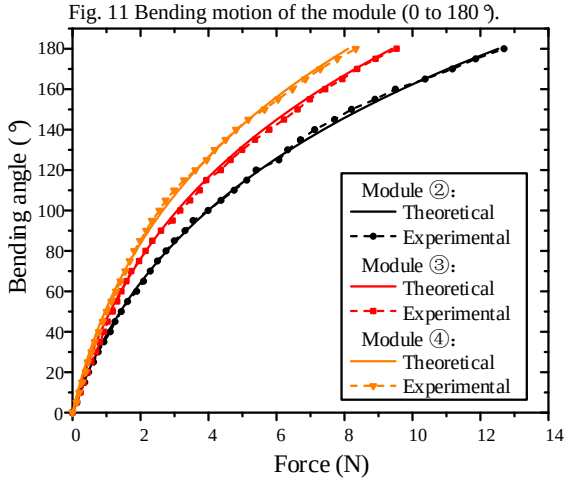

Fig. 12. Experiment results of the bending motion of module ②, ③, ④.

B. *Experiment on manipulators*

Different modules can be assembled into a series manipulator. The manipulator Ⅰ is assembled by the modules ②, ③ and ④. The manipulator Ⅱ is assembled by the modules ③, ⑤ and ⑥. The above platform is also applied to test the kinematics of the two manipulators. Cables are fixed to the end of the manipulator through all the 3 sections. The bending motion processes of two manipulators are shown in fig.13. Both the manipulators can reach a bending angle more than 270 °.The experiment results of the manipulator Ⅰ and manipulator Ⅱ are shown in fig.14 and fig.15, respectively. Within the range from 0 to 270 °, the maximum error of manipulator Ⅰ and Ⅱ are 4. 43 °, 4.71 °, respectively. The error does not exceed 5 °.

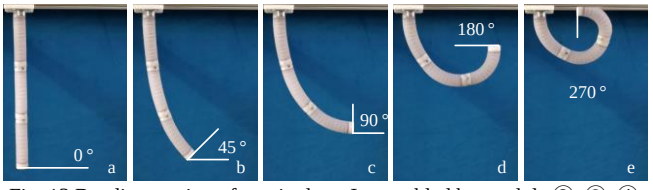

Fig. 13 Bending motion of manipulator I assembled by module ②, ③, ④.

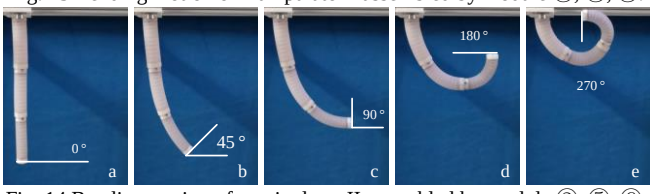

Fig. 14 Bending motion of manipulator II assembled by module ③, ⑤, ⑥.

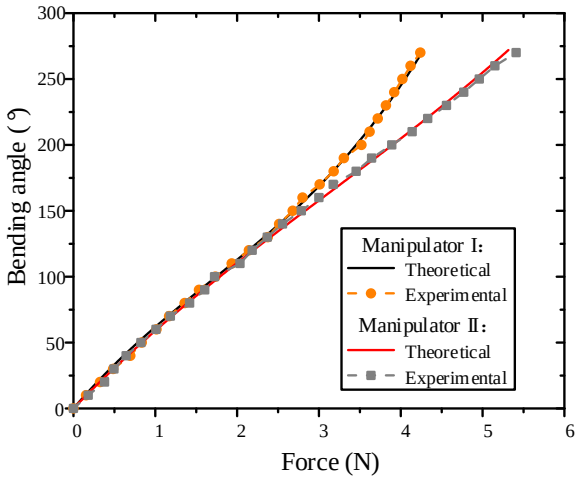

Fig.15. Experiment results of the two manipulators.

C. *Experiments on the gripper*

As shown in fig.16, a gripper is assembled by three modules. The module's length is 80mm and the diameter is 14mm. Three modules are symmetrically fixed on a 3D printed base. The module is mounted diagonally on the base to grab larger objects. The weight of the gripper is 68g.

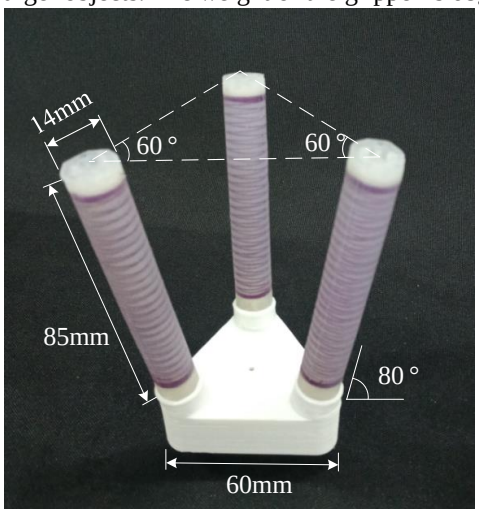

Fig.16. The gripper equipped with three modules.

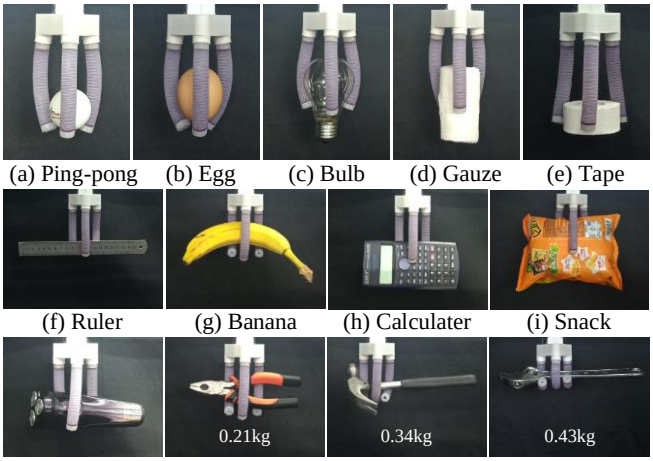

(a) Ping-pong (b) Egg (c) Bulb (d) Gauze (e) Tape

(f) Ruler (g) Banana (h) Calculater (i) Snack

(j) Razor (k) Vise (l) Hammer (m) Spanner

Fig.17. Grasping of different objects by the gripper.

The gripper can grasp different shapes of objects and fragile items such as bulbs and eggs. And it also can lift heavy items such as a hammer or a spanner. The results also demonstrate the good flexibility, adaptability and load capacity of the module. This rigid-flexible coupled design method of adding a spring into soft module can be a very simple and effective way to enhance its practical application.

D. Discussion

As can be observed from the experiment results, the motion of the module and the manipulator confirms to the kinematic model. The reason is summarized in two point. One is to consider the friction of cable and the gravity of the module. In particular, the friction is a kind of non-linear force that increases exponentially as the bending angle increase. Another is the rigidity of the module is increased after the spring is added. The deformation of the module is more uniform and stable. The bending curve is closer to an arc. This idea of design and the kinematics model may help the precise control of the soft manipulator. Moreover, the soft module embedded with spring performs good flexibility, adaptability and load capacity. The spring can improve the stiffness of the soft module while it is not sacrifice the softness and flexibility.

V. CONCLUSION

This paper proposes a rigid-flexible coupled cable-driven soft module design, which has the characteristics of compact structure, light weight, good stiffness, flexible and large range of motion. The spring can improve the stiffness and motion stability of the module. The rigid connectors at both ends of the module realize the plug-and-connect connection between the modules. And through the extension design of the modules are introduced to achieve series manipulator with multiple modules of different sizes, and separate curvature control for each section. Then the kinematics model of the module and the tandem manipulator is established based on the PCC model. In order to ensure the accuracy of kinematics, the friction of the cables and the gravity of the module are introduced into the model. The maximum bending angle of the modules is 180 °, and the maximum bending angle of the manipulators is more than 270 °. The modules and the manipulators can perform good accuracy within the range of bending motion. the maximum error of modules ②, ③, ④are 2.41 °, 2.35 °, 2.46 °, respectively. The error does not exceed 2.5 °. And the maximum error of manipulator Ⅰ and Ⅱ are 4.71 °, 4.43 °, respectively. The error does not exceed 5 °. The results have verified the effectiveness of the kinematics. Finally a gripper equipped with three modules can grasp many items with different shapes, sizes, roughness and weights. It also demonstrate the good flexibility, adaptability and load capacity of the module.

REFERENCES

[1] M Manti, V Cacucciolo, M Cianchetti. Stiffening in Soft Robotics: A Review of the State of the Art[J]. IEEE Robotics & Automation Magazine, 2016, vol. 23, no. 3, pp.93-106.

[2] Rich, I Steven, J W Robert, and M Carmel. "Untethered soft robotics." Nature Electronics 2018, vol. 1, no. 2, pp.102-112.

[3] A Rafsanjani, K Bertoldi, A R Studart. Programming Soft Robots with Flexible Mechanical Metamaterials[J]. Science Robotics, 2019, vol. 4, no. 29, pp.1-3.

[4] F. Renda, M. Cianchetti, M. Giorelli, et al, "A 3D steady-state model of a cable-driven continuum soft manipulator inspired by the octopus arm," Bioinspiration & Biomimetics, 2012, vol. 7, 025006.

[5] F. Renda, M. Giorelli, M. Calisti, et al, "Dynamic Model of a Multibending Soft Robot Arm Driven by Cables," IEEE Transactions on Robotics, 2014, vol. 30, pp.1109-1122.

[6] Y. Ansari, M. Manti, E. Falotico, et al, "Towards the development of a soft manipulator as an assistive robot for personal care of elderly people," 2017, vol. 14, pp.291-301.

[7] M. Cianchetti, R. Tommaso, G Giada, et al, "Soft robotics technologies to address shortcomings in today's minimally invasive surgery: the STIFF-FLOP approach," Soft robotics, 2014, vol.1 pp. 122-131.

[8] A. Arezzo, Y. Mintz, ME. Allaix, et al, "Total mesorectal excision using a soft and flexible robotic arm: a feasibility study in cadaver models," Surgical Endoscopy, 2016, vol. 31, pp. 1-10.

[9] MA. Robertson, A. Matthew, and J. Paik, "New soft robots really suck: Vacuum-powered systems empower diverse capabilities," Science Robotics, 2017, vol. 2, eaan6357.

[10] F. Renda, F. Boyer, J. Dias, et al. "Discrete Cosserat Approach for Multi-Section Soft Robots Dynamics," unpublished.

[11] H Wang, C Wang, X Liang, and et al. "Three-dimensional dynamics for cable-driven soft manipulator," IEEE/ASME Transactions on Mechatronics 2017, vol. 22, pp. 18-28.

[12] SP. Timoshenko, "Strength of Materials[M]," 1940.